



1 **Phylogeography and population genetics of the European mudminnow**
2 **(*Umbra krameri*) with a time-calibrated phylogeny for the family Umbridae**

3

4 Saša Marić¹, David Stanković^{2,3}, Josef Wanzenböck⁴, Radek Šanda⁵, Tibor Erős⁶, Péter
5 Takács⁶, András Specziár⁶, Nenad Sekulić⁷, Doru Bănăduc⁸, Marko Čaleta⁹, Ilya Trombitsky¹⁰,
6 Laslo Galambos¹¹, Sandor Sipos¹², Aleš Snoj^{2*}

7

8 ¹ *Institute of Zoology, Faculty of Biology, University of Belgrade, Studentski trg 16, 11001*
9 *Belgrade, Serbia*

10 ² *Department of Animal Science, Biotechnical Faculty, University of Ljubljana, Groblje 3, SI-*
11 *1230 Domžale, Slovenia*

12 ³ *Department of Life Sciences, University of Trieste, Via Licio Giorgieri 5, 34127 Trieste, Italy*

13 ⁴ *Research Institute for Limnology, University of Innsbruck, Mondseestraße 9, 5310 Mondsee,*
14 *Austria*

15 ⁵ *National Museum, Department of Zoology, Václavské náměstí 68, 115 79 Prague 1, Czech*
16 *Republic;*

17 ⁶ *Balaton Limnological Institute, MTA Centre for Ecological Research, Klebelsberg Kuno u.*
18 *3, H-8237 Tihany, Hungary*

19 ⁷ *Institute for Nature Conservation of Serbia, Dr Ivana Ribara 91, 11070 Novi Beograd, Serbia*

20 ⁸ *Faculty of Sciences, Lucian Blaga University of Sibiu, Dr. Ion Rațiu 5-7, RO-550012, Sibiu,*
21 *Romania*

22 ⁹ *Faculty of Teacher Education, University of Zagreb, Savska cesta 77, 10000 Zagreb, Croatia*

23 ¹⁰ *Eco-TIRAS International Association of Dniester River Keepers, Teatrala 11A, Chisinau*
24 *2012, Moldova*

25 ¹¹ *Institute for Nature Conservation of Vojvodina, Radnička 20a, 21000 Novi Sad, Serbia*

26 ¹² *Department of Biology and Ecology, Faculty of Science, University of Novi Sad, Trg D.*
27 *Obradovića 2, Novi Sad, Serbia*

28

29

30 * Corresponding author: Aleš Snoj

31 Telephone number: 00 386 1 3203 912

32 Fax number: 00 386 1 3203 888

33 E-mail: ales.snoj@bf.uni-lj.si

34

35

36

37

38

39

40

41

42

43 **Abstract**

44 The genetic structure of European mudminnow populations throughout the species range was examined using
45 mitochondrial DNA and seven microsatellite loci. Ten mitochondrial haplotypes were detected, suggesting three
46 phylogeographic lineages, which likely diverged during the Early and Middle Pleistocene. These three lineages
47 geographically correspond to three regions: the Danube drainage including the Drava system and Dniester Delta,
48 the Sava system, and the Tisza system. High genetic diversity observed using mtDNA was confirmed with
49 microsatellite data, suggesting the existence of 14 populations in the studied area. The isolation-with-migration
50 model showed that migration rates between populations were generally low, and were highest between the Drava
51 and its tributary Mura. According to the inferred relative population splitting times, *U. krameri* likely spread from
52 the eastern part of the species range to the west, which also showed the highest genetic diversity and largest
53 population size. As reported by the time-calibrated phylogeny, separation of the European and American *Umbra*
54 occurred roughly at the end of Late Cretaceous and in the first half of the Paleogene (60.57 Ma with 95% highest
55 probability density of 39.57 – 81.75). Taking these results into account, appropriate guidelines are proposed to
56 conserve European mudminnow populations.

57

58 **Key words:** *Umbra krameri*, Umbridae, mtDNA, Microsatellites, Time-calibrated phylogeny, Conservation

59

60 **Introduction**

61 Longitudinal and transverse damming of rivers has altered water flows and the habitats of many freshwater fish
62 species, and is often considered a major cause of the freshwater fish biodiversity crisis (Abell, 2002; Cambray,
63 1997). Transverse damming is performed for power generation and to improve navigation conditions, whereas
64 longitudinal damming is usually tied to flood control and re-claiming arable land. In lowland landscapes, the
65 predominantly longitudinal damming of rivers has intersected formerly vast wetlands and marshes associated with
66 larger rivers, dramatically altering the landscape. Wetland and marsh adapted species have been particularly
67 affected by these changes, and previously vast habitats have been largely diminished, leading to dramatic
68 population declines and local extinctions (Olden, 2016).

69 A notable example is seen in the European mudminnow (*Umbra krameri* Walbaum, 1792), a fish
70 specifically adapted to the margins of lowland rivers, floodplains and marshes (Bănărescu & Bănăduc, 2007;
71 Bănărescu et al., 1995; Pekárik et al., 2014; Wanzenböck, 1995, 2004). *U. krameri* could serve as a focal species
72 for this specific type of threatened ecosystem (Lambeck, 1997; Mace et al., 2007) or as indicator species for

73 ecosystem function (Wanzenböck, 2004). It has a relatively small distribution area restricted to the lowlands of
74 the Danube and Dniester drainages. Its populations are believed to be declining in many countries (Mikschi &
75 Wanzenböck, 1995; Bănăduc, 2008); though some previously unrecorded populations have recently been reported
76 (Govedič, 2010; Sekulić et al., 2013; Trombitsky et al., 2001; Velkov et al., 2004; unpublished data). They are
77 located scattered in small floodplain pools, oxbow lakes and marshy wetlands. During floods, populations may be
78 interconnected, allowing for genetic exchange in a metapopulation framework (Akçakaya et al., 2007).

79 *U. krameri* has been listed as a vulnerable (VU) species by the IUCN (Freyhof, 2013) and is strictly
80 protected under the Bern convention (Appendix II), and protected by the EU Habitats Directive 92/43/EEC (listed
81 in Annex II) and the national legislation in most countries in its range. While legal protection is guided
82 internationally, conservation efforts are generally localized and are often not coordinated at the national level.
83 Ideally, conservation planning should be performed irrespective of social and administrative entities (i.e. countries
84 or provinces), and should address biologically meaningful spatial scales. This starts with the strategic
85 consideration of conservation management at the spatial scale of the total distribution range, and should be
86 successively broken down into smaller spatial scales such as river basins, sub-basins and river stretches.
87 Particularly rare genotypes may deserve higher conservation priority overriding other spatial considerations
88 (Moritz et al., 2002).

89 Along with *U. krameri*, the family Umbridae includes four other species according to the traditional
90 taxonomy (Umbridae *sensu lato*): the central mudminnow (*U. limi*), eastern mudminnow (*U. pygmaea*), Olympic
91 mudminnow (*Novumbra hubbsi*) and Alaska blackfish (*Dallia pectoralis*), all populating North America, with the
92 latter also extending into northeast Siberia (Kuehne & Olden, 2014).

93 Genetic studies of the Umbridae are relatively scarce; molecular phylogeny of the family has been
94 primarily studied in the context of higher evolutionary ranks regarding Esociformes and Salmoniformes (e.g.
95 Campbell et al., 2013; López et al., 2000; López et al. 2004; Shedko et al., 2013). These studies revealed that
96 North American and European representatives of *Umbra* (*U. limi*, *U. pygmaea* and *U. krameri*) are monophyletic
97 (1), while *Umbra*, *Dallia* and *Novumbra* form a paraphyletic group (2), where *Dallia* and *Novumbra* are actually
98 in monophyly with *Esox* (3). Therefore, it was suggested that the family Umbridae should only contain the genus
99 *Umbra* and the closely related fossil genera *Boltyshia*, *Paleoesox* and *Proumbra* (Umbridae *sensu* Gaudant, 2012),
100 while the family Esocidae should also contain *Dallia* and *Novumbra* along the genus *Esox* (Campbell et al., 2013).

101 Phylogeographic and/or population genetic studies have been performed on *Dallia* (Campbell & López,
102 2014; Campbell et al., 2014a), *N. hubbsi* (Pickens, 2003; Adams et al., 2013; DeHaan et al., 2014) and on *U.*

103 *krameri* at a limited scale in Serbia, Bosnia-Herzegovina and Hungary (Marić et al., 2015; Takács et al., 2015).
104 Contrary to *N. hubbsi*, which was found to be genetically homogeneous at the mitochondrial DNA level, *Dallia*
105 and *U. krameri* populations showed extensive phylogeographic structuring.

106 In this study we analyse the genetic structure of *U. krameri* using mitochondrial (cytochrome b) and
107 nuclear (tetranucleotide microsatellites) markers (Winkler & Weiss, 2009) throughout most of its range – the
108 Danubian drainage including its major systems, the Drava, Tisza and Sava Rivers, and the Dniester River Delta.
109 This analysis aims to give a comprehensive overview of the phylogeography and population genetics of the
110 species, while also providing fundamental guidelines for its conservation.

111 In previous phylogenetic studies of the genus *Umbra*, all three species were not studied together to
112 produce a time-calibrated phylogeny. For that reason, the evolutionary relationship of these three taxa was also
113 examined to infer a time-calibrated phylogeny for the family Umbridae.

114

115 **Materials and methods**

116 Sampling and DNA isolation

117 A total of 341 specimens were collected using electrofishing and wattle baskets (Sekulić et al., 2013) from 17
118 locations across the Danube drainage and the Dniester Delta (Fig. 1; Table 1), from 2011 to 2015. Fin clips were
119 sampled and stored in 96% ethanol. Total DNA was isolated using the phenol-chloroform-isoamyl alcohol method
120 (Sambrook et al., 1989) or DNeasy Blood and Tissue kit (Qiagen, Germany) as per manufacturer instructions.
121 Samples from the five Hungarian populations (Sződ-Rákospatak, Kolon-tavi-övesatorna, Ricsei-csatorna, Hejő
122 and Zala) were previously used in a population genetics study of *U. krameri* in the Hungarian part of the
123 Carpathian Basin (Takács et al., 2015), while two specimens from the Lower Sava (Gromiželj and Bakreni Batar)
124 and one from the Middle Danube (Lugomir) were previously used in a study on the genetic and morphological
125 variability of *U. krameri* in Serbia and Bosnia and Herzegovina (Marić et al., 2015).

126

127 Mitochondrial DNA

128 The mitochondrial protein-coding gene cytochrome b (entire length of 1141 bp) was PCR-amplified in 182
129 individuals (Table 1) using GluF and ThrR primers and the PCR conditions as described in Machordom &
130 Doadrio (2001). Both-directional sequencing was carried out on an ABI Prism 3130xl DNA sequencer using the
131 same primers. DNA sequences were edited and aligned using the programs Chromas Lite 2.01
132 (<http://www.technelysium.com.au/chromas.html>; Technelysium Pty Ltd, Australia) and Clustal X (Thompson et

133 al., 1997). Mean genetic net-distances between phyletic lineages were calculated in the program MEGA 5 (Tamura
134 et al., 2011), using the Kimura two-parameter model (Kimura, 1980). The cytochrome b sequences obtained in
135 this study were deposited in GenBank (accession numbers KP898868 – KP898876 and KU674836). The
136 genealogical relations between haplotypes were presented as a minimum spanning network (MSN) using the 95%
137 statistical parsimony criterion in the TCS 1.2 program (Clement et al., 2000). Phylogenetic and molecular clock
138 analysis were performed in BEAST v 1.8.3 (Drummond et al., 2012) using the Birth-Death Process (Gernhard,
139 2008), uncorrelated lognormal relaxed clock (Drummond et al., 2006), TN93 substitution model (Tamura & Nei,
140 1993) and gamma-shaped rate variation (Yang, 1993) and run online on the CIPRES Science Gateway portal v.
141 3.3 (Miller et al., 2010); the substitution model was selected with ModelGenerator (Keane et al., 2006) based on
142 the Aikake Information Criterion (AIC; Akaike, 1974).

143 For molecular clock analysis, the dataset was expanded with cyt b sequences of other Esociformes
144 deposited in GenBank (Table 2). As no appropriate calibration dates are available for the *Umbra* genus, fossil
145 records of other Esociformes were used to calibrate the molecular clock. For the minimum age of all Esociformes,
146 *Esteesox*, a stem esociform from the late Cretaceous (85 Ma, Wilson et al., 1992) was used, while *Esox kronneri*
147 Grande, 1999, the first record of the subgenus *Kenoza* from the late early Eocene (42 Ma, Grande, 1999) was used
148 as a minimum bound for the divergence between *Esox lucius* and *E. niger*. For both fossil calibrations, the
149 lognormal priors recommended by Campbell et al. (2013) were applied: the prior for all Esociformes had an offset
150 of 85.0 with a mean of 1.0 and a SD of 1.0 (5% CI – 85.5, 95% CI – 99.1), and the prior for the split within *Esox*
151 had an offset of 42.0 with a mean of 1.0 and SD 0.65 (5% CI – 45.9, 95% CI – 52.9). Calculations were conducted
152 using the BEAGLE library (Ayres et al., 2012) and run in three independent runs of 30,000,000 generations
153 sampled every 3000 generations. After verifying adequate sampling (ESS > 200) and convergence with Tracer
154 (Rambaut et al., 2014), a 10% burn-in was applied and the tree files were combined with LogCombiner. Finally,
155 TreeAnnotator was used to calculate a maximum clade credibility tree, median values of divergence times,
156 posterior probabilities, and bounds for the 95% highest posterior density (HPD) interval.

157 Microsatellites

158 Seven microsatellite loci (*UkrTet1*, *UkrTet3–UkrTet8*) were amplified in 341 individuals (Table 1), according to
159 previously published protocols (Winkler & Weiss, 2009). Fragment analysis was performed on a 3130xl Genetic
160 Analyzer and genotyped using Gene-Mapper v4.0 (Applied Biosystems).

161 The presence of null alleles, gene diversity (heterozygosity), F-statistics, as well as inter-population allele
162 sharing distances (D_{AS}), were calculated for all populations using Microchecker v2.2.3 (Van Oosterhout et al.,

163 2004), GENETIX 4.04 (Belkhir et al., 1996–2004), FSTAT 2.9.3.2 (Goudet, 2002) and Populations software
164 (Langella, 2002), respectively. Private alleles and allelic richness were estimated by rarefaction analysis, using
165 ADZE (Szpiech et al., 2008), to compare genetic diversity among populations despite unequal sample numbers
166 and to assess whether sampling effort was sufficient to capture genetic diversity. To determine whether stepwise-
167 like mutations have contributed to genetic differentiation (Hardy et al. 2003), allele size (R_{ST}) and the allele
168 identity-based measure (F_{ST}) were compared by testing whether the observed R_{ST} was larger than the value
169 obtained after permuting allele sizes among alleles within populations (pR_{ST}) as implemented in SPAGeDI 1.3
170 (Hardy & Vekemans 2002; 20,000 permutations).

171 Genetic differentiation of the whole sample set was assessed using hierarchical STRUCTURE analysis
172 (Pritchard et al., 2000; Vähä et al., 2007). STRUCTURE 2.3.2.1 runs Markov chain Monte Carlo (MCMC)
173 simulations to partition individuals into K clusters. For runs estimating $\ln \Pr(X|K)$ under a certain K , different run
174 lengths were used (from 20,000 to 100,000 burn-in and 100,000 to 500,000 total length, repeated seven times for
175 each K) depending on convergence. Stepwise exclusion of the most differentiated clusters was conducted in the
176 hierarchical STRUCTURE analysis, allowing for more precise clustering of the remaining individuals without
177 eliminating admixed individuals. Each excluded cluster was investigated for possible hidden substructures by
178 choosing K values according to each specific setting (Vähä et al., 2007). The ΔK method (Evanno et al., 2005)
179 was applied to estimate the most probable K (Appendix 1 in Supplementary Material).

180 In order to determine the amount of gene-flow between populations and to estimate the parameter theta
181 (θ), the isolation-with-migration model (IM, as implemented in the software IMA2; Hey & Nielsen, 2007) was
182 used. Mitochondrial cytochrome b gene and microsatellite loci were analysed together. The HKY model of
183 sequence evolution was applied to mitochondrial sequences, and a stepwise mutation model (SMM) was assumed
184 for microsatellite loci. IM was applied to all neighbouring populations and to several additional combinations
185 selected on the basis of the results from the STRUCTURE analysis (total of 23 combinations; all tested populations
186 are listed in Appendices 2, 3 and 4 in the Supplementary Material). Five parameters were estimated for each
187 combination: current and ancestral population sizes (θ_1 , θ_2 and θ_{ANC} , respectively), relative time since divergence
188 (t) and a single migration parameter (m). Upper bounds for parameter priors were estimated for each tested
189 population pair from consecutive preliminary runs of the program, based on initial estimates of θ as advised in the
190 IMA2 manual and span: -q (30 – 400), -m (0.75 – 4), -t (4 – 30). In all combinations, 100 Markov chains were run
191 in parallel under a geometric heating scheme. Several shorter trial runs with different heating schemes were
192 explored between selection of population pairs (6) to identify high swapping rates between adjunct chains. The

193 settings ($h_a = 0.99$, $h_b = 0.3$) gave adequate swapping rates (40% to 80% between the majority of adjunct chains),
194 and resulted in good mixing of the Markov chains for all tested population pairs. For the final simulations, the
195 manual recommendations for large datasets were followed. For each tested combination, two independent jobs
196 were run until a suitable burn-in was reached for at least 1,000,000 steps. Next, a new set of runs was started by
197 reloading the Markov chain state file with an additional short burn-in period of 100,000 steps and afterwards
198 20,000 genealogies were sampled every 50 steps from a total 1,000,000 steps. Both Markov chain state files
199 generated in burn-in runs were used two times. Finally, all four replicates were combined in L-mode run with
200 identical parameter settings. Based on the 1.3 ± 0.5 average age of maturity (Kuehne & Olden, 2014), migration
201 events were assessed using a generation time of two years.

202

203 **Results**

204 **MtDNA analysis**

205 Aligned sequences of the 1085 bp 3'-end cytochrome b mtDNA gene obtained from 182 individuals grouped into
206 ten haplotypes: Da1 and Sa1 were previously identified in the Danube and Sava drainages in Serbia and Bosnia-
207 Herzegovina (Marić et al., 2015), while the remaining haplotypes (i.e. Da2, Da3, Da4, Da5, Da6, Da7, Ti1 and
208 Ti2) were not previously described. The haplotypes Da1, Da2 and Da3 were found predominantly in the Upper
209 and Middle Danube, Da4 and Da5 were detected only in the Danube Delta. Da6, the most frequent and widespread
210 haplotype was restricted to the Drava River system, Lake Balaton, the Lower Danube River and the Dniester
211 Delta, but was completely lacking in the Upper and Middle Danube. Da7 was detected only in the Dniester Delta,
212 Ti1 and Ti2 only in the Tisza River system in Hungary. Sa1 was detected in the Sava River system and in the
213 Danube River, though only in proximity to the Sava mouth (Table 1).

214 The phylogenetic reconstruction of the mitochondrial haplotypes as inferred from the Bayesian tree (Fig.
215 2) supports the monophyly of the *Umbra* genus and the sister relationship between *U. limi* and *U. pygmaea* (López
216 et al, 2000; López et al. 2004). *U. krameri* clustered into two clades: one was statistically well supported (0.97
217 posterior probability) and comprised of very similar haplotypes found in the Drava, Balaton, Danube and Dniester
218 locations (Danube phyletic lineage), while the second showed only weak support (0.47 posterior probability). This
219 less supported clade is formed by two phyletic lineages, represented by two haplotypes detected only in the Tisza
220 River (Tisza phyletic lineage), and a haplotype detected primarily in the Sava River sites (Sava phyletic lineage).
221 Mean net-distances between the three lineages were 0.003 between the Danube and Tisza phyletic lineages, 0.006
222 between the Danube and the Sava phyletic lineages and 0.005 between the Tisza and the Sava phyletic lineages.

223 MSN (Fig. 1) supported the topology represented by the Bayesian tree (Fig. 2) and revealed the central
224 position of the haplotype Da6 as being one or two mutation steps from the other Da haplotypes, four mutations
225 from the Ti1 and Ti2 haplotypes, and six from the Sa1 haplotype.

226 The molecular clock analysis based on the alignment of ten *U. krameri* haplotypes and six other
227 Umbirdae and Esocidae species with two calibration points (*Estesox* for Esociformes and *E. kronneri* for the first
228 record of the subgenus *Kenoza*) yielded a divergence time for the European and American *Umbra* species of 60.57
229 Ma (with a 95% highest probability density (HPD) of 39.57–81.75 Ma), while the diversification within *U.*
230 *krameri* was estimated to start at 1.01 Ma (with 95% HPD of 0.48–1.74) (Fig. 2). The Tisza + Sava lineages first
231 separated from the Danubian ones, followed by the splitting of the Sava and Tisza lineages at 0.70 Ma (with 95%
232 HPD of 0.19–0.90).

233

234 Microsatellite DNA analysis

235 Rarefaction analysis revealed allelic richness that varied from 3.4 to 11.1 and observed heterozygosity varied from
236 0.331 to 0.819, with the highest values observed in Enisala (Danube Delta) and the Dniester Delta, and the lowest
237 in Šuma Žutica (Sava) (Table 1). Rarefaction analysis showed that the private allelic richness in populations from
238 both deltas (0.64 in the Danube and 1.63 in the Dniester) did not decrease with an increasing number of individuals
239 (Fig. 3a; Table 1). Furthermore, certain population group combinations (between Lower Danube & Dniester,
240 Upper & Middle Danube, Drava & Balaton, Sava and Tisza; Table 1) showed that the Lower Danube & Dniester
241 – Tisza combination exhibited the highest private allele sharing, closely followed by the combinations Sava –
242 Lower Danube & Dniester, Lower Danube & Dniester – Drava & Balaton, and Upper & Middle Danube – Lower
243 Danube & Dniester (Fig. 3b). Neither null alleles nor deviations from Hardy-Weinberg equilibrium were detected
244 in the examined populations.

245 The degree of differentiation among the 17 analysed populations was significant and relatively high in
246 most cases, and spanned from 0.022–0.514 for pairwise F_{ST} and 0.108–0.915 for D_{AS} (Table 3).

247 In the hierarchical STRUCTURE analysis, the most probable numbers of K values were K=2 for the 1st
248 and 3rd steps and K=5 for both 2nd steps (for details see Appendix 1 in Supplementary Material). In accordance
249 with these K values, European mudminnows were partitioned into two groups in the first step: the Upper and
250 Middle Danube (Lugomir and upstream locations), Mura, Drava and Balaton (group I), and the Sava, Tisza,
251 Middle and Lower Danube (Kraljevac and downstream locations) and Dniester Delta, (group II). In further steps,
252 additional partitioning within both groups became evident; in group I in the Upper and Middle Danube, each

253 sampling site represented a genetically well-defined homogeneous population. The Drava (Županijski kanal) and
254 Balaton (Zala) population showed some inter-population genetic mixing with the genetically similar population
255 from the Mura River (Nagy Parlag). In group II, Comana (Lower Danube) and Šuma Žutica (Sava) formed distinct
256 and well defined homogeneous populations. Populations from the Lower Sava (Bakreni Batar and Gromiželj) and
257 from the Middle Danube near the mouth of the Sava (Kraljevac) represented an admixture of two distinct genetic
258 units. Within the group of remaining locations, Palanca-Mayaki (Dniester) and Ricsei-csatorna (Tisza) were
259 genetically homogeneous and distinctive, while individuals from the Hejő (Tisza) and Enisala (Danube Delta)
260 exhibited admixed genotypes derived from the previous two populations. Further intra-population partitioning did
261 not reveal any additional clusters (Fig. 4, Appendix 1 in Supplementary Material).

262 The observed R_{ST} value of the whole sample set was 0.436, while the pR_{ST} value was 0.151 ($P = 0.0000$)
263 and the F_{ST} value was 0.207. The significantly higher R_{ST} than pR_{ST} , and considerably higher value than F_{ST} ,
264 suggested that SMM contributed to genetic differentiation; furthermore, no non-tetra nucleotide repeat motifs
265 were observed. IM analysis of neighbouring populations revealed a stepping-stone pattern with low levels of
266 migration (Fig. 5, Appendix 3 and 4 in Supplementary material). In the majority of tested population pairs, runs
267 produced clear peaks and replicates resulted in similar estimates of all parameters. An arbitrary value of 0.05 for
268 the bin with the highest value in the migration histogram (HiPt) was used to identify migration rates greater than
269 zero. The strongest migration paths were observed between Mura (Nagy Parlag) and Drava (Županijski kanal)
270 and between the Middle Danube (Kraljevac) and Lower Sava (Gromiželj and Bakreni Batar joined). When
271 converting the migration parameter into per-generation population migration rates ($M = \theta \times m/2$), peak locations
272 corresponded to 2.61 ($M_{MUR} \rightarrow M_{DRA}$) and 0.56 ($M_{DRA} \rightarrow M_{MUR}$) migration events per generation between Mura
273 and Drava and to 1.12 ($M_{M.DAN} \rightarrow M_{L.SAV}$) and 3.35 ($M_{L.SAV} \rightarrow M_{M.DAN}$) events between the Middle Danube and
274 Lower Sava. This suggests 1.31 or 0.28 migration events per year between the Mura and Drava and 0.56 or 1.68
275 events between the Middle Danube and Lower Sava when taking into account the average European mudminnow
276 generation time (two years). Within the Danubian watershed, migrations were generally higher in the Middle and
277 Upper Danube and in the Sava, Tisza and Drava-Balaton watersheds than in the Lower Danube. Only negligible
278 migration was detected between Comana and Enisala, while migration rate between the Lower (Comana) and the
279 Middle Danube (Kraljevac) were very small. The IM model also revealed no trans-watershed migrations between
280 the Sava and Drava and Middle Danube and Tisza, while low levels of migrations were detected between the
281 Danube Delta (Enisala) and the Upper Tisza (Ricsei-csatorna). Migration rates between the Danube Delta and the
282 Upper Tisza correspond to 0.09 ($M_{D.DAN} \rightarrow M_{U.TIS}$) and 1.83 ($M_{U.TIS} \rightarrow M_{D.DAN}$) migration events per year.

283 The IM model showed that Enisala (Danube Delta) and Palanca-Mayaki (Dniester Delta) populations
284 were the largest, with θ values of 44.78 and 25.10, respectively, followed by the Hejő (Middle Tisza; $\theta = 12.09$)
285 and Kraljevac (Middle Danube; $\theta = 8.37$), while Šuma Žutica (Middle Sava) was the smallest population with the
286 lowest theta value ($\theta = 0.40$). In the Županijski kanal (Drava; $\theta = 5.87$), considerable variation was observed in
287 the θ estimation between the tested population pairs (Table 1 and Appendix 2 in Supplementary Material). In
288 addition, the relative times since divergence calculated by the IM model were generally older in the eastern range
289 of the species, especially when comparing the Enisala population (Danube Delta) to other populations (Appendix
290 3 in Supplementary Material).

291

292 **Discussion**

293 Phylogeography and molecular clock analysis of *U. krameri*

294 The phylogenetic mtDNA analysis of the extensive sample-set, which covered the majority of the *U. krameri*
295 range, revealed three phyletic lineages that corresponded closely to three main rivers in the area: Danube, Sava
296 and Tisza.

297 Diversification within *U. krameri* started at approximately 1.01 Ma (0.48 – 1.74), which is in general
298 agreement with the time frame set by Marić et al. (2015), who proposed that the Sava lineage separated from the
299 Danubian lineage approximately 0.70 Ma ago. The time span of the presumed diversification of the species
300 includes two Pleistocene glaciations (Günz and the first phase of Mindel) (Gibbard & van Kolfschoten, 2004;
301 Penck & Brückner, 1909). Although the areas inhabited by these mudminnow populations were not covered with
302 ice sheets (Mangerud et al. 2004), indirect effects of glacial events could have shaped the river network of the
303 middle Danube. Furthermore, intensive tectonic movements occurred in the same period, which may have resulted
304 in significant shifts of river courses within the basin (Brilly, 2010). Thus, the palaeogeological events of the Early
305 and Middle Pleistocene could have played a significant role in shaping the genetic differentiation of *U. krameri*,
306 likely separating the Sava and the Tisza populations from the Danube-Mura-Drava-Balaton populations, and
307 initiating their genetic divergence.

308 As mudminnow can thrive only in a narrow range of environmental conditions and is sensitive to
309 competition, in addition to major Pleistocene geological events, even simple random habitat fragmentation may
310 have led to population isolation and lineage formation.

311 The most frequently observed haplotype (Da6) was also the most widespread, and was found in the most
312 distant sites of the species range, i.e. in the Mura River in the west, and the Dniester Delta in the east. Also, Da6

313 appeared to be the central and presumably the ancestral haplotype of the entire species. Yet, its modern distribution
314 is patchy; its occurrence in the Drava River and relative proximity to Lake Balaton is expected and likely reflects
315 Late Pleistocene communication between the two systems, as proposed by Gábris & Mari (2007). The question
316 arises as to why this haplotype is lacking in the Upper and Middle Danube, where it is substituted with its
317 derivatives (Da1-Da3) and why it is again abundant in the Lower Danube and Dniester Delta. Considering that *U.*
318 *krameri* is a habitat specialist, and also that mtDNA has a higher level of genetic drift than nuclear DNA markers,
319 the most likely explanation for the patchy distribution of Da6 haplotype appears to be genetic drift.

320

321 Time-calibrated phylogeny for Umbridae family

322 This phylogenetic analysis confirmed the paraphyly of the Umbridae family (*Umbra*, *Novumbra*, *Dallia*), placing
323 *Novumbra* and *Dallia* within the Esocidae (Campbell et al., 2013, Gaudant, 2012, Shedko et al., 2013) and
324 confirming the monophyly of the genus *Umbra* (López et al., 2000, 2004). Previous phylogenetic studies of the
325 Umbridae family did not examine all three *Umbra* species together to produce a time calibrated phylogeny (c.f.
326 Campbell et al., 2013; López et al., 2000, 2004; Shedko et al., 2013), and thus the time of the split between the
327 North American and European *Umbra* was not resolved. According to the time-calibrated phylogeny presented
328 here, *Umbra* separated from the rest of the Esociformes approximately at the end of the Early or in the Late
329 Cretaceous, which is comparable to the time estimation in Campbell et al. (2013), while the separation of the
330 European and American *Umbra* species roughly spans the end of the Late Cretaceous into the first half of the
331 Paleogene. During that period, the Atlantic Ocean was already well formed, separating Eurasia and North America
332 (Scotese, 2001), thus this estimate places the split between the European and American *Umbra* much later than at
333 the breakup of the Laurasian supercontinent. The molecular results presented here indicate that the split between
334 the North American and European *Umbra* pre-dates the oldest known fossil representative of the genus *Umbra*,
335 collected in Northern Bohemia and dating to the Late Oligocene (*U. prochazkai* Oberhlová, 1978), making
336 ancestral *Umbra* a contemporary of the oldest known fossil representative of the Umbridae family (*sensu* Gaudant,
337 2012) collected in the Boltyska basin of Ukraine and dating to the late Palaeocene (*Boltysia brevicauda*
338 Sytchevskaya & Daniltschenko, 1975). The split between the North American and European *Umbra* is decidedly
339 deeper than the split between the subgenera *Kenoza* and *Esox* and is comparable to the split between the genera
340 *Novumbra* and *Esox* in terms of the molecular clock analysis. Therefore, differences between the North American
341 and European *Umbra* could well be interpreted at the genus level; or at least, classification into the subgenus
342 *Melanura* (Agassiz, 1853) as defined by Nelson (1972) should be followed.

343 Based on the time-calibrated phylogeny presented in this study, the distribution of ancestral *Umbra* might
344 have extended bi-continently either across the North Atlantic Land Bridge (NALB) and/or the Beringia Land
345 Bridge (BLB), which linked the continents across the Atlantic and the Pacific oceans and were available
346 intermittently from the beginning of the Paleocene (Brikiatis, 2014), with final subsidence of the NALB during
347 the late Miocene (Denk et al., 2011; Tiffney, 1985) and loss of the BLB near the end of the Pleistocene (Gladenkov
348 et al., 2002). However, given that the native distribution of *Umbra* in North America (subgenus *Melanura*) is
349 exclusive to the Atlantic drainage, and that the distribution of *Umbra* in Eurasia (subgenus *Umbra*) is restricted
350 to Central Europe and the Black Sea watershed (including the fossil record), the distribution of a once common
351 ancestor most likely extended across the North Atlantic Land Bridge. Furthermore, a lack of fossils from the
352 family Umbridae (*sensu* Gaudant, 2012) from North America indicates that the genus may have originated in
353 Europe. A similar biogeographic origin and distribution pattern between sister lineages was recently described for
354 the freshwater fish genera *Sander* (Haponski & Stepien, 2013) and *Perca* (Stepien et al. 2015), where North
355 American and European sister lineages diverged much later than the breakup of Laurasia and coincided with the
356 closure of the NALB during the Miocene. The examples of *Sander* and *Perca* clearly demonstrate that such
357 biogeographic scenarios are also possible with freshwater fish.

358

359 Population genetics and demography of *U. krameri*

360 Although the results of the mtDNA analysis of *U. krameri* showed a considerable level of genetic variation
361 observable through the clustering of haplotypes into three phylogeographic lineages, analysis of microsatellite
362 loci allowed for a more precise resolution of genetic variation. Namely, the pairwise F_{ST} values (Table 3) revealed
363 a strongly significant statistical difference between 16 of the 17 sampled locations, with the exception of Bakreni
364 Batar and Gromiželj (Lower Sava), where mudminnows were recognized as a uniform population. In addition to
365 this pair, STRUCTURE analysis did not separate populations from Županijski kanal (Drava) – Zala (Lake
366 Balaton) and Enisala (Danube Delta) – Hejő (Lower Tisza). Therefore, the Danube watershed and Dniester Delta
367 harbour at least 14 genetically differentiated populations of *U. krameri*.

368 Regarding the population pairs from the Lower Sava (Bakreni Batar – Gromiželj) and from the Drava
369 and Lake Balaton (Županijski kanal – Zala), the genotype clustering results are not surprising, as respective pairs
370 were physically connected until recently (Gábris & Mari, 2007; Marić et al., 2015). This is also supported by the
371 shared haplotypes (Sa1 and Da6, respectively) (Table 1). However, the relationship between the two deltas
372 (especially Danube Delta) and the Middle Tisza population remains puzzling. Although these three populations

373 are geographically very distant, and though the populations from both deltas share no haplotypes with the Tisza
374 population, microsatellite analysis suggested their similarity. But even so, the IM model showed no migration
375 between them, which suggests that the apparent genetic similarity is likely a consequence of ancestral
376 polymorphism rather than gene flow. This assumption is congruent with the fact that ancestral alleles persist
377 longer in large populations, such as Enisala, Palanca-Mayaki and Hejő, the three largest populations in this study.
378 Furthermore, large effective population sizes can lead also to allelic saturation. If so, similar allelic frequency
379 profiles may not indicate recent extensive genetic exchange or retention of ancestral polymorphisms, but could
380 reflect size homoplasy leading to misinterpretations of long-term relationships (Estoup et al., 2002).

381 A strong genetic spatial structure is also reflected by the inferred migration pattern. The IM approach
382 detected a stepping-stone migration pattern with low levels of migration. Converted per-generation population
383 migration rates generally correspond to the migration of less than one individual per generation (Appendix 4, in
384 Supplementary Material). In general, migration was higher in the Middle and Upper Danube and in the Sava,
385 Tisza and Drava-Balaton watersheds and lower in the Lower Danube. As discussed above, the only population
386 where no migration with neighbouring populations was observed was Palanca-Mayaki in the Dniester Delta. This
387 absence of gene-flow between the Dniester and the Danube Delta excludes a migration pathway through the Black
388 Sea, a speculation originating from the observation of the species in the Black Sea (Raykov et al. 2012), which
389 was most likely false (Hajdú et al. 2015). In addition, the IM model revealed no trans-watershed migration
390 between the Sava and Drava and Middle Danube and Tisza, while low levels of migration were detected between
391 the Danube Delta (Enisala) and the Upper Tisza (Ricsai-csatorna). Although a connection between these two
392 populations could theoretically be explained by ancestral polymorphism, this is highly unlikely, as the IM
393 approach distinguishes between potential ancestral polymorphism and recurrent contemporary gene flow
394 occurring after population separation (Marko & Hart, 2012). However, genetic similarity due to size homoplasy
395 associated with mutation-driven saturation effects cannot be excluded. Not considering the cluster joining the
396 Danube Delta and Hejő population, the STRUCTURE analysis largely coincided with the results from the IM
397 approach and confirmed higher gene-flow within the identified clusters (e.g. between Patašký kanál and Kolon-
398 tavi-övcatorna within the Drava-Balaton watershed).

399 Takács et al. (2015) estimated similar but somewhat higher migration rates between mudminnow
400 populations from the Carpathian basin using MIGRATE-N. Direct comparison is difficult, as Takács et al. (2015)
401 pooled their samples according to the STRUCTURE analysis despite large distances between sampling sites. They
402 reported the highest rates (>1.5 individuals per generation) between the Middle Hungarian Region (including

403 Kolon-tavi-övcSATORna) and Hanság-Szigetköz in the Middle Danube, from Balaton to Mura in the Drava-Balaton
404 watershed, and from Middle Tisza including the Köros River watershed to the Upper Tisza. The different
405 migration rates detected between these studies are likely due to the use of different migration estimation software.
406 While MIGRATE-N assumes that the size and the population structure have been stable for $\sim 4 N_{ef}$ generations,
407 IMA2 does not make this assumption and thus is well suited for the analysis of younger populations (reviewed in
408 Kuhner, 2009). Therefore, when the ratio between N_{ef} and the splitting time is high, MIGRATE-N cannot
409 distinguish between gene flow and shared ancestral polymorphism, leading to an overestimation of migration rates
410 (Marko & Hart, 2012). Furthermore, population subdivision can affect migration rate estimates (Wakeley et al.,
411 2000).

412

413 Defining units for conservation purposes

414 In comparing the genetic diversity of *U. krameri* (Table 1) and its counterparts *D. pectoralis* and *N. hubbsi* in
415 North America (Campbell et al., 2014a; DeHaan et al., 2014), the highest allelic richness was detected in the
416 lowest reaches of the largest rivers in all three species. The populations from the Danube and Dniester deltas
417 displayed the highest microsatellite diversity and the largest effective population sizes. Such large differences in
418 θ between these two populations and those from other locations can be attributed to the wide range of habitats in
419 the Danube and Dniester deltas in comparison with upstream locations; e.g. the Danube Delta which covers a vast
420 area of approximately 4,152 km², also had the highest number of detected mtDNA haplotypes (4 of 10; Table 1),
421 with the central Da6 haplotype as dominant (Fig. 1). Furthermore, both deltas and the entire Lower Danube are
422 the only areas where private allelic richness increased with sample size (Fig. 3a). Exceptional parameters of
423 genetic polymorphism and high effective population sizes in both deltas indicate that the eastern part of the species
424 range should be considered the centre of the species diversity. Rich genetic diversity in deltas could be attributed
425 to the stochastic dynamics typical of large populations, where the effects of genetic drift is minor compared to
426 small populations, causing allelic richness to increase with sample size. The population divergences estimated
427 using the IM model showed that the splits between neighbouring populations were oldest in the eastern part of the
428 range. This suggests a possible expansive role of habitats in the delta regions, from where *U. krameri* likely spread
429 to the west (i.e. to the remaining sampling area) and not vice versa. This is also supported by the shared private
430 alleles (mean number of private alleles for major population cluster combinations) found in the Upper and Middle
431 Danube from the Lower Danube & Dniester and in the Tisza, Sava, Drava & Balaton, (Fig. 3b).

432 Mitochondrial DNA analysis revealed some genetic divergence among three geographically well-defined
433 groups, the Tisza, Sava and Danube (mean net-distances between them were from 0.003 to 0.006), indicating a
434 certain period of their distinct evolution (see discussion above). This is also supported by the estimation of inter-
435 population gene-flow, which was minimal among those three groups, suggesting considerable reproductive
436 isolation. For these reasons, these three phyletic lineages, as defined by the three haplogroups, could be considered
437 potential evolutionary significant units (ESU). On the other hand, the uneven distribution of microsatellite
438 polymorphism among the small sampled populations and high genetic structuring within each of the three phyletic
439 lineages may not reflect a natural evolutionary process but rather random drift governed by recent habitat
440 fragmentation as a result of human impact (e.g., damming). For example, the smallest population with the lowest
441 genetic diversity was detected in an isolated locality in the Sava river system (Šuma Žutica) in Croatia (Table 1)
442 covering just a few square kilometres, with no other known records of *U. krameri* in the region. Adaptive
443 differentiation seems unlikely in very recently split populations with small N_e , as there is simply no time for
444 selection to take place. In cases like this, it is questionable whether such small populations represent genetically
445 viable entities with a good prospect of long-term survival. Therefore, caution should be taken when delineating
446 ESUs on the basis of microsatellites, as these markers known for their high mutation rate and neutral evolutionary
447 history are likely to result in excessive splitting of populations (Frankham et al., 2012) and are generally
448 inadequate for characterizing adaptive patterns (Funk et al., 2012).

449

450 **Acknowledgments**

451 This study received support from the Slovenian Research Agency, the Ministry of Education, Science and
452 Technological Development of the Republic of Serbia (Grant No. 173045) and the SYNTHESYS Project (CZ-
453 TAF-5090; <http://www.synthesys.info/>) financed by European Community Research Infrastructure Action under
454 the FP7 Integrating Activities Programme. RŠ was supported by the Ministry of Culture of the Czech Republic
455 (DKRVO 2016/15, National Museum, 00023272) and DS by the DIANET postdoctoral fellowship programme
456 (FP1527385002). TE, PT and ASp would like to express their thanks for Eszter Csoma for the DNA extraction of
457 the Hungarian samples. Many thanks to dr Ladislav Pekarik for collected samples of European mudminnow from
458 the Slovak Republic.

459

460 **References**

461 Abell, R., 2002. Conservation biology for the biodiversity crisis: A freshwater follow-up. *Conservation Biology*
462 16: 1435–1437.

463 Adams, B., P. W. DeHaan, R. Tabor, B. Thompson & D. K. Hawkins, 2013. Characterization of tetranucleotide
464 microsatellite loci for Olympic mudminnow (*Novumbra hubbsi*). *Conservation Genetics Resources* 5: 573–
465 575.

466 Agassiz, L., 1853. Recent researches of Prof. Agassiz. *American Journal of Science and Arts (Ser. 2)* 16: 134–
467 136.

468 Akaike, H., 1974. A new look at the statistical model identification. *IEEE Transactions on Automatic Control* 19:
469 716–723.

470 Akcakaya, H. R., G. Mills & C. P. Doncaster, 2007. The role of metapopulations in conservation. In Macdonald,
471 D. W. & K. Service (eds), *Key topics in conservation biology*. Blackwell Publishing, Oxford: 64–84.

472 Ayres, D. L., A. Darling, D. J. Zwickl, P. Beerli, M. T. Holder, P.O. Lewis, J. P. Huelsenbeck, F. Ronquist, D. L.
473 Swofford, M. P. Cummings, A. Rambaut & M. A. Suchard, 2012. BEAGLE: An application programming
474 interface and high-performance computing library for statistical phylogenetics. *Systematic Biology* 61:
475 170–173.

476 Bănăduc, D., 2008. *Umbra krameri* Walbaum, 1792 a Natura 2000 protected fish species, in Romania. *Acta*
477 *Ichtiologica Romanica* 3: 33–44.

478 Bănărescu, P. M., V. Otel & A. Wilhelm, 1995. The present status of *Umbra krameri* Walbaum in Romania.
479 *Annalen des Naturhistorischen Museums in Wien* 97B: 496–501.

480 Bănărescu, P. M. & D. Bănăduc, 2007. Habitats Directive (92/43/EEC) fish species (Osteichthyes) on the
481 Romanian territory. *Acta Ichtiologica Romanica* 2: 43–78.

482 Belkhir, K., P. Borsa, L. Chikhi, N. Raufaste & F. Bonhomme, 1996–2004. GENETIX v. 4.04, Logiciel sous
483 Windows™ pour la Génétique des Populations. Université Montpellier 2, Laboratoire Génome et
484 Population, Montpellier.

485 Brilly, M., 2010. *Hydrological Processes of the Danube River Basin: Perspectives from the Danubian Countries*.
486 Springer, New York.

487 Brikiatis, L., 2014. The De Geer, Thulean and Beringia routes: key concepts for understanding early Cenozoic
488 biogeography. *Journal of Biogeography* 2014: doi:10.1111/jbi.12310.

489 Cambay, J., 1997. Freshwater fish- a global biodiversity crisis. *Hydrobiologia* 353: 199–202.

490 Campbell, M. A., J. A. López, T. Sado & M. Miya, 2013. Pike and salmon as sister taxa: Detailed intraclade
491 resolution and divergence time estimation of Esociformes + Salmoniformes based on whole mitochondrial
492 genome sequences. *Gene* 530: 57–56.

493 Campbell, M. A. & J. A. López, 2014. Mitochondrial phylogeography of a Beringian relict: the endemic
494 freshwater genus of blackfish *Dallia* (Esociformes). *Journal of Fish Biology* 84(2): 523–538.

495 Campbell, M. A., G. K. Sage, R. L. DeWilde, J. A. López & S. L. Talbot, 2014a. Development and
496 characterization of 16 polymorphic microsatellite loci for the Alaska blackfish (Esociformes: *Dallia*
497 *pectoralis*). *Conservation Genetics Resources* 6(2): 349–351.

498 Clement, M., D. Posada & K. Crandall, 2000. TCS: a computer program to estimate gene genealogies. *Molecular*
499 *Ecology* 9: 1657–1660.

500 DeHaan, P. W., B. A. Adams, R. A. Tabor, D. K. Hawkins & B. Thompson, 2014. Historical and contemporary
501 forces shape genetic variation in the Olympic mudminnow (*Novumbra hubbsi*), an endemic fish from
502 Washington State, USA. *Conservation Genetics* 15: 1417–1431.

503 Denk, T., Grimsson, F., Zetter, R., Simonarson, L. A. 2011. The biogeographic history of Iceland – the North
504 Atlantic Land Bridge revisited. *Topics in Geobiology* 35: 647–668.

505 Drummond, A. J., S. Y. W. Ho, M. J. Phillips & A. Rambaut, 2006. Relaxed phylogenetics and dating with
506 confidence. *PLoS Biology* 4: e88. doi:10.1371/journal.pbio.0040088.

507 Drummond, A. J., M. A. Suchard, D. Xie & A. Rambaut, 2012. Bayesian phylogenetics with BEAUti and the
508 BEAST 1.7. *Molecular Biology and Evolution* 29: 1969–1973.

509 Estoup, A., P. Jarne & J.-M. Cournet, 2002. Homoplasy and mutation model at microsatellite loci and their
510 consequences for population genetics analysis. *Molecular Ecology* 11: 1591–1604.

511 Evanno, G., S. Regnaut & J. Goudet, 2005. Detecting the number of clusters of individuals using the software
512 STRUCTURE: a simulation study. *Molecular Ecology* 14: 2611–2620.

513 Felsenstein, J., 1985. Confidence limits on phylogenies: An approach using the bootstrap. *Evolution* 39: 783–791.

514 Frankham, R., J. D. Ballou, M. R. Dudash, M. D. B. Eldridge, C. B. Fenster, R. C. Lacy, J. R. Mendelson, I. J.
515 Porton, K. Ralls & O. A. Ryder, 2012. Implications of different species concepts for conserving
516 biodiversity. *Biological Conservation* 153: 25–31.

517 Freyhof, J., 2013. *Umbra krameri*. The IUCN Red List of Threatened Species. Version 2014.2.
518 <www.iucnredlist.org>. Downloaded on 11 November 2014.

- 519 Funk, W. C., J. K. McKay, P. A. Hohenlohe & F. W. Allendorf, 2012. Harnessing genomics for delineating
520 conservation units. *Trends in Ecology and Evolution* 27(9): 489–496.
- 521 Gábris, Gy. & L. Mari, 2007. The Pleistocene beheading of the Zala River (West Hungary). *Földrajzi értesítő* 56:
522 39–50. [In Hungarian with an English summary].
- 523 Gaudant, J., 2012. An attempt at the palaeontological history of the European mudminnows (Pisces, Teleostei,
524 Umbridae). *Neues Jahrbuch Fur Geologie Und Palaontologie-Abhandlungen* 263(2): 93–109.
- 525 Gernhard, T., 2008. The conditioned reconstructed process. *Journal Theoretical Biology* 253: 769–778.
- 526 Gibbard, P. & T. van Kolfschoten, 2004. The Pleistocene and Holocene epochs. In Gradstein, F. M., J. G. Ogg &
527 A. G. Smith (eds), *A Geologic Time Scale*. Cambridge University Press, Cambridge: 441–452.
- 528 Gladenkov, A. Y., A. E. Oleinik, L. Marinovich & K. B. Barinov, 2002. A refined age for the earliest opening
529 of Bering Strait. *Palaeogeography Palaeoclimatology Palaeoecology* 183: 321–328.
- 530 Goudet, J., 2002. FSTAT, a program to estimate and test gene diversities and fixation indices (version 2.9.3.2).
531 <http://www2.unil.ch/popgen/softwares/fstat.htm>. Accessed 15 October 2009.
- 532 Govedič, M., 2010. Ribe reke Drave med Mariborom in Hrvaško mejo 35 let po izgradnji hidroelektrarn [Fish of
533 Drava river between Maribor and Croatian border 35 years after construction of hydro power plants]. In
534 Book of Abstracts–International conference on the Drava River–Life in the river basin, Slovenia,
535 Dravograd (30. 09. – 01. 10. 2010.). Jovan Hadži Institute of Biology Scientific Research Centre SASA,
536 Municipality Dravograd, RRA Koroška–Regional Development Agency for Koroška, Ljubljana–
537 Dravograd: 22–23.
- 538 Grande, L., 1999. The first *Esox* (Esocidae: Teleostei) from the Eocene Green River Formation, and a brief review
539 of esocid fishes. *Journal of Vertebrate Paleontology* 19: 271–292.
- 540 Hajdú, J., L. Várkonyi, J. Ševc & T. Müller, 2015. Corrective notice to the European mudminnow (*Umbra krameri*
541 Walbaum, 1792) record from the Black Sea. *Biologia* 70: 1429–1431.
- 542 Hardy, O. J, N. Charbonnel, H. Freville & M. Heuertz, 2003. Microsatellite allele sizes: a simple test to assess
543 their significance on genetic differentiation. *Genetics* 163: 1467–1482.
- 544 Hardy, O. J. & X. Vekemans, 2002. SPAGeDi: a versatile computer program to analyse spatial genetic structure
545 at the individual or population levels. *Molecular Ecology Notes* 2: 618.
- 546 Hey, J. & R. Nielsen, 2007. Integration within the Felsenstein equation for improved Markov Chain Monte Carlo
547 methods in population genetics. *Proceedings of the National Academy of Sciences* 104: 2785–2790.

548 Jombart, T. & I. Ahmed, 2011. Adegenet 1.3-1: new tools for the analysis of genome-wide SNP data.
549 Bioinformatics 27: 3070–3071.

550 Jombart, T., S. Devillard & F. Balloux, 2010. Discriminant analysis of principal components: a new method for
551 the analysis of genetically structured populations. BMC Genetics 11: 94.

552 Keane, T. M., C. J. Creevey, M. M. Pentony, T. J. Naughton & J.O. McInerney, 2006. Assessment of methods for
553 amino acid matrix selection and their use on empirical data shows that ad hoc assumptions for choice of
554 matrix are not justified. BMC Evolutionary Biology 6: 29. doi: 10.1186/1471-2148-6-29.

555 Kimura, M., 1980. A simple method for estimating evolutionary rates of base substitutions through comparative
556 studies of nucleotide sequences. Journal of Molecular Evolution 16: 111–120.

557 Kuehne, M. L. & D. J. Olden, 2014. Ecology and conservation of mudminnow species worldwide. Fisheries 39:
558 341–351.

559 Kuhner, M. K., 2009. Coalescent genealogy samplers: windows into population history. Trends in Ecology and
560 Evolution 24: 86–93.

561 Lambeck, R. J., 1997. Focal species: A multi-species umbrella for nature conservation. Conservation Biology 11:
562 849–856.

563 Langella, O., 2002. Populations 1.2.28. Logiciel de génétique des populations. Laboratoire Populations, génétique
564 et évolution, CNRS UPR 9034, Gif-sur-Yvette. <http://www.cnrs-gif.fr/pge/>. Accessed 10 October 2009.

565 López, A., Bentzen, P., Pietsch, W., 2000 Phylogenetic relationships of Esocoid fishes (Teleostei) based on partial
566 cytochrome b and 16S mitochondrial DNA sequences. Copeia 2: 420-431.

567 López, A., Chen, W., Ortí, W., 2004. Esociform phylogeny. Copeia 3: 449– 464.

568 Mace, G. M., H. P. Possingham & N. Leader-Williams, 2007. Prioritizing choices in conservation. In Macdonald,
569 D.W. & K. Service (eds), Key topics in conservation biology. Blackwell Publishing, Oxford: 17–34.

570 Machordom, A. & I. Doadrio, 2001. Evidence of a Cenozoic Betic-Kabilian connection based on freshwater fish
571 phylogeography (*Luciobarbus*, Cyprinidae). Molecular Phylogenetics and Evolution 18: 252–263.

572 Marić, S., A. Snoj, N. Sekulić, J. Krpo-Ćetković, R. Šanda & V. Jojić, 2015. Genetic and morphological variability
573 of the European mudminnow *Umbra krameri* (Teleostei, Umbridae) in Serbia and in Bosnia and
574 Herzegovina – a basis for future conservation activities. Journal of Fish Biology 86(5): 1534–1548.

575 Marko, P. B. & M. W. Hart, 2012. Retrospective coalescent methods and the reconstruction of metapopulation
576 histories in the sea. Evolutionary Ecology 26: 291–315.

577 Mangerud, J., M. Jakobsson, H. Alexanderson, V. Astakhov, G. K. C. Clarke, M. Henriksen, C. Hjort, G. Krinner,
578 J. Lunkka, P. Möller, A. Murray, O. Nikolskaya, M. Saarnisto & J. Svendsen, 2004. Ice-dammed lakes and
579 rerouting of the drainage of northern Eurasia during the Last Glaciation. *Quaternary Science Reviews* 23:
580 1313–1332.

581 Mikschi, E. & J. Wanzenböck, 1995. Proceedings of the First International Workshop on *Umbra krameri*. *Annalen*
582 *des Naturhistorischen Museums in Wien* 97B: 438–508.

583 Miller, M. A., W. Pfeiffer & T. Schwartz, 2010. Creating the CIPRES Science Gateway for inference of large
584 phylogenetic trees. In *Proceedings of the Gateway Computing Environments Workshop (GCE)*, 14 Nov.
585 2010. New Orleans: 1–8.

586 Moritz, C., K. McGuigan & L. Bernatchez, (2002). Conservation of freshwater fishes: integrating evolution and
587 genetics with ecology. In: Collares-Pereira, M. J., I. G. Cowx & M. M. Coelho (eds), *Conservation of*
588 *Freshwater Fishes: Options for the Future*. Oxford: Fishing News Books, Blackwell Science: 293–310.

589 Nelson, G. J., 1972. Cephalic sensory canals, pitlines, and the classification of esocoid fishes, with notes on
590 galaxiids and other teleosts. *American Museum Novitates* 2492: 1–49.

591 Olden, J. D., 2016. Challenges and opportunities for fish conservation in dam-impacted waters. In: Closs, G. P.,
592 M. Krkosek & J. D. Olden (eds), *Conservation of Freshwater Fishes*. Cambridge University Press: 107-
593 142.

594 Pekárik, L., J. Hajdú & J. Koščo, 2014. Identifying the key habitat characteristics of threatened European
595 mudminnow (*Umbra krameri*, Walbaum 1792). *Fundamental and Applied Limnology* 184: 151–159.

596 Penck, A. & E. Brückner, 1909. *Die Alpen im Eiszeitalter*. Taunitz, Leipzig.

597 Pickens, D. C., 2003. Genetic evidence for a population bottleneck in the Olympic mudminnow (*Novumbra*
598 *hubbsi*). B.S. Degree, University of Puget Sound, Tacoma.

599 Pritchard, J. K., M. Stephens & P. Donnelly, 2000. Inference of population structure using multilocus genotype
600 data. *Genetics* 155: 945–959.

601 Rambaut, A., M. A. Suchard, D. Xie & A. J. Drummond, 2014. Tracer v1.6, Available from
602 <http://beast.bio.ed.ac.uk/Tracer>

603 Raykov, V. St., M. Panayotova, P. Ivanova, I. Dobrovolov & V. Maximov, 2012. First record and allozyme data
604 of European mudminnow *Umbra krameri* Walbaum, 1792 (Pisces: Umbridae) in the Black Sea. *Comptes*
605 *rendus de l'Académie bulgare des Sciences* 65(1): 49–52.

606 R Development Core Team, 2009. R: A language and environment for statistical computing. R Foundation for
607 Statistical Computing, Vienna, Austria. ISBN 3-900051-07-0, URL. <<http://www.R-project.org>>.
608 Downloaded on 11 September 2014.

609 Sambrook, J., E. F. Fritseh & T. Maniatis, 1989. Molecular Cloning. A Laboratory Manual, 2nd edn. NY: Cold
610 Spring Harbor Laboratory Press, Cold Spring Harbor.

611 Scotese, C. R., 2001. Atlas of Earth History, Volume 1, Paleogeography, PALEOMAP Project, Arlington.

612 Sekulić, N., S. Marić, L. Galamboš, D. Radošević & J. Krpo-Četković, 2013. New distribution data and population
613 structure of the European mudminnow *Umbra krameri* in Serbia and Bosnia and Herzegovina. Journal of
614 Fish Biology 83: 659–666.

615 Shedko, S. V., I. L. Miroshnichenko & G. A. Nemkova, 2013. Phylogeny of Salmonids (Salmoniformes:
616 Salmonidae) and its molecular dating: analysis of mtDNA data. Russian Journal of Genetics 49: 623–637.

617 Szpiech, Z. A., M. Jakobsson & N. A. Rosenberg, 2008. ADZE: a rarefaction approach for counting alleles private
618 to combinations of populations. Bioinformatics: 24, 2498–2504.

619 Takács, P., T. Erős, A. Specziár, P. Sály, Z. Vitál, Á. Ferincz, T. Molnár, Z. Szabolcsi, P. Bíró & E. Csoma, 2015.
620 Population genetic patterns of threatened European Mudminnow (*Umbra krameri* Walbaum, 1792) in a
621 fragmented landscape: implications for conservation management. PLoS ONE 10(9): e0138640.

622 Tamura, K. & M. Nei, 1993. Estimation of the number of nucleotide substitutions in the control region of
623 mitochondrial DNA in humans and chimpanzees. Molecular Biology and Evolution 10: 512–526.

624 Tamura, K., D. Peterson, N. Peterson, G. Stecher, M. Nei & S. Kumar, 2011. MEGA5: molecular evolutionary
625 genetics analysis using maximum likelihood, evolutionary distance, and maximum parsimony methods.
626 Molecular Biology and Evolution 28: 2731–2739.

627 Thompson, J. D., T. J. Gibson, F. Plewniak, F. Jeanmougin & D. G. Higgins, 1997. The CLUSTAL_X windows
628 interface, flexible strategies for multiple sequence alignment aided by quality analysis tool. Nucleic Acids
629 Research 25: 4876–4882.

630 Tiffney, B. H., 1985. The Eocene North Atlantic Land Bridge: its importance in Tertiary and modern
631 phytogeography of the Northern Hemisphere. Journal of the Arnold Arboretum 66: 243–273.

632 Trombitsky, I., V. Lobcenco & A. Moshu, 2001. The European mudminnow, *Umbra krameri*, still populates the
633 Dniester River in Moldova. Folia Zoologica 50: 159–160.

634 UNESCO, World Heritage List, Danube Delta. <<http://whc.unesco.org/en/list/588>>. Downloaded on 13 August
635 2014.

636 Vähä, J. P., J. Erkinaro, E. Niemelä & C. R. Primmer, 2007. Life-history and habitat features influence the within-
637 river genetic structure of Atlantic salmon. *Molecular Ecology*, 16: 2638–2654.

638 Van Oosterhout, C., W. F. D. Hutchinson, P. M. Wills & P. Shipley, 2004. MICRO-CHECKER: software for
639 identifying and correcting genotyping errors in microsatellite data. *Molecular Ecology Notes* 4: 535–538.

640 Velkov, B., L. Pehlivanov & M. Vassilev, 2004. *Umbra krameri* (Pisces: Umbridae): A reinstated species for the
641 Bulgarian ichthyofauna. *Acta Zoologica Bulgarica* 56: 233–235.

642 Wakeley, J., 2000. The effects of subdivision on the genetic divergence of populations and species. *Evolution* 54:
643 1092–1101.

644 Wanzenböck, J., 1995. Current knowledge on the European mudminnow *Umbra krameri* Walbaum, 1792.
645 *Annalen des Naturhistorischen Museums in Wien* 97B, 439–449.

646 Wanzenböck, J., 2004. European mudminnow (*Umbra krameri*) in the Austrian floodplain of the River Danube –
647 Conservation of an indicator species for endangered wetland ecosystems in Europe. In Akcakaya, H. R.,
648 M. A. Burgman, O. Kindvall, C. C. Wood, P. Sjögren-Gulve, J. S. Hatfield & M. A. McCarthy (eds),
649 *Species Conservation and Management*. Oxford University Press, New York: 200–207.

650 Wilson, M. V. H., D. B. Brinkman & A. G. Neuman, 1992. Cretaceous Esocoidae (Teleostei): early radiation of
651 the pikes in North American fresh waters. *Journal of Paleontology* 66: 839–846.

652 Winkler, K. A. & S. Weiss, 2009. Nine new tetranucleotide microsatellite DNA markers for the European
653 mudminnow *Umbra krameri*. *Conservation Genetics* 10: 1155–1157.

654 Yang, Z., 1993. Maximum likelihood estimation of phylogeny from DNA sequences when substitution rates differ
655 over sites. *Molecular Biology and Evolution* 10: 1396–1401.

656

657 **Figure captions**

658 **Fig. 1** Main diagram: Map of sampling locations. Names and codes of sampling locations are reported in Table 1,
659 with square pie charts representing the distribution and frequencies of mtDNA haplotypes. The Danube and the
660 Dniester drainage area are delineated with thick dotted lines, while the borders between sub-drainages are shown
661 with thin dotted lines. The Drava and the Lake Balaton subdrainages are joined together as they were connected
662 and formed a single drainage until the Late Pleistocene. Lower left: The genealogical haplotype network of
663 European mudminnow. Haplotypes are connected with lines that, regardless of length, represent a single mutation.
664 Black circles represent missing or theoretical haplotypes. Haplotype colours correspond to the square pie charts
665 in the central diagram.

666 **Fig. 2** Fossil calibrated phylogeny of Esociformes generated using a relaxed clock in BEAST. 95% HPD intervals
667 are shown as violet bars at nodes. Median node ages are shown as node labels. The upper left square shows the
668 same Bayesian phylogenetic tree with branch lengths representing substitutions, the scale bar indicates the number
669 of substitutions per site, and posterior probabilities are shown as node labels.

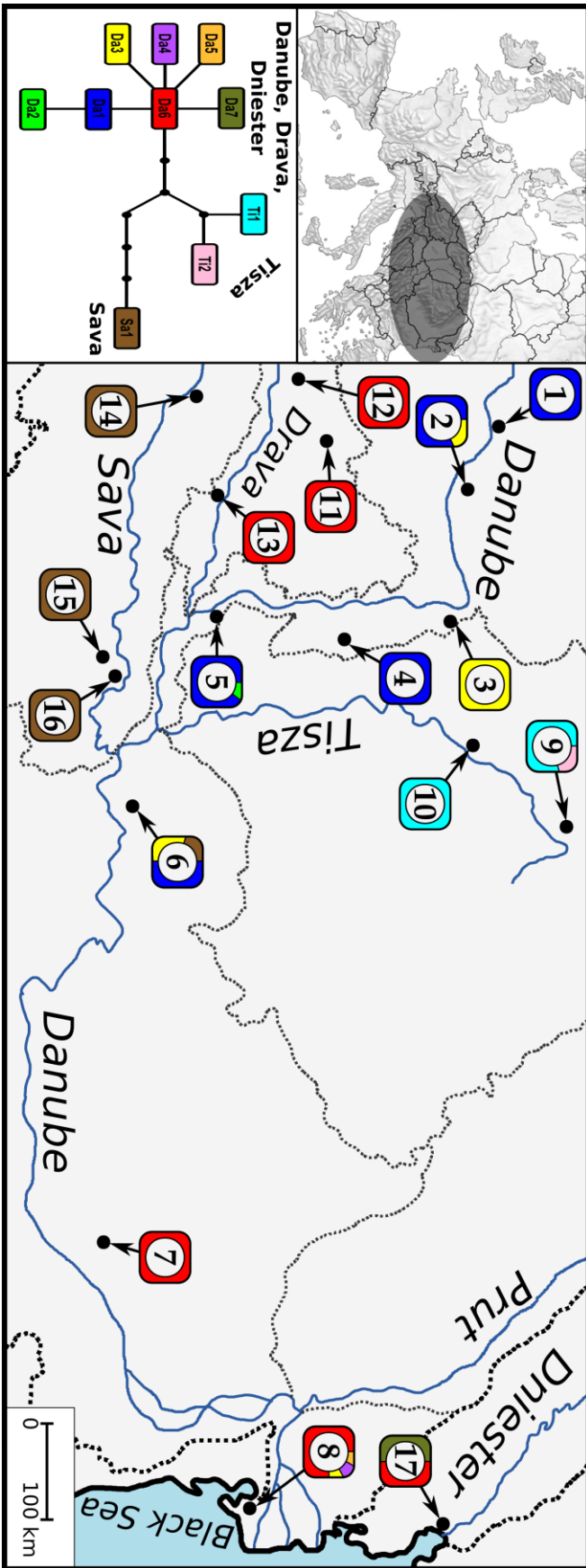
670 **Fig. 3** Rarefaction analysis of private alleles for five major clusters as inferred from geography and population
671 analysis (a), and rarefaction analysis of shared private alleles for combinations of major population clusters (b).
672 Upper & Middle Danube (locations 1-6; Table 1), Lower Danube & Lower Dniester (locations 7, 8 and 17), Tisza,
673 Sava including Kraljevac in the Middle Danube, and Drava & Balaton including Mura.

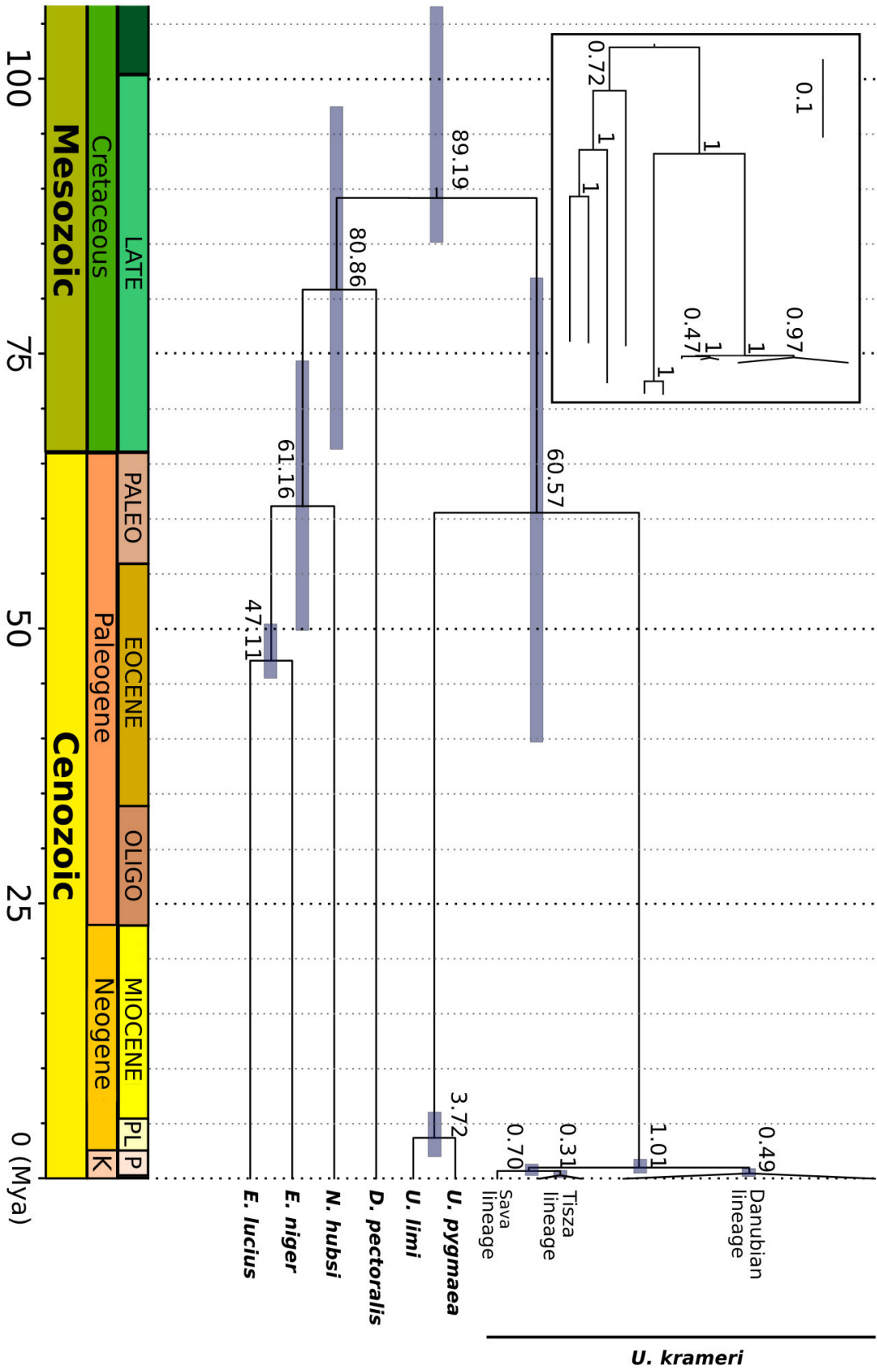
674 **Fig. 4** Estimated population structure as inferred by hierarchical STRUCTURE analysis of microsatellite marker
675 DNA data. Black lines separate sampling sites. After three steps, 14 clusters were identified. The most probable
676 K for the analysed samples shown in the arrows is based on the ΔK method; no further structures were detected
677 in subsequent rounds (after the third step) and within the excluded clusters ($K=1$). Arrows delineate the progress
678 of the hierarchical approach, where subsets of the data were subsequently analysed.

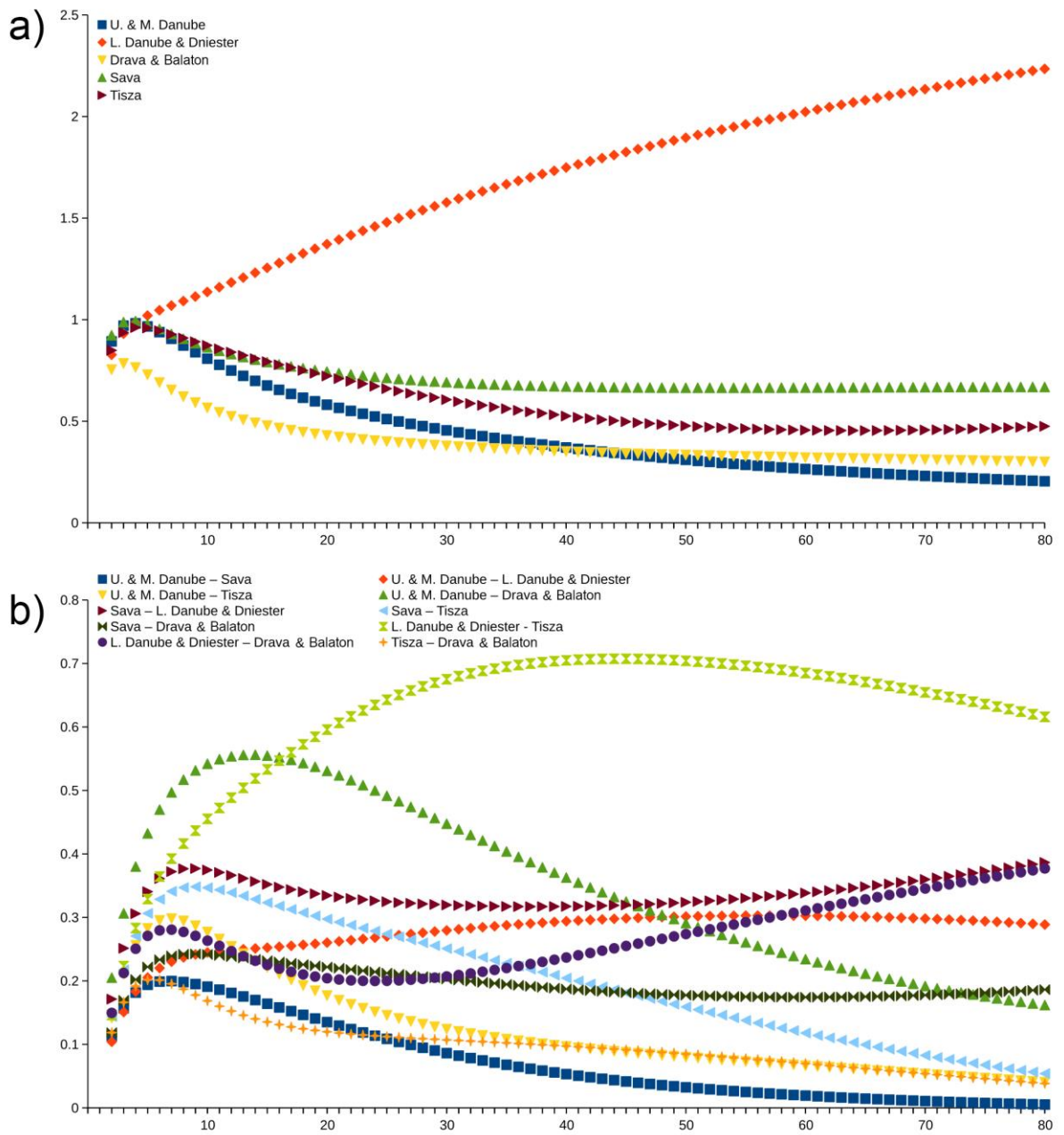
679 **Fig. 5** Migration patterns according to IM model estimates. Arrow width corresponds to IMA2's HiPt estimate of
680 migration rate as presented in the legend (upper left). Only migration rates above 0.05 are shown; see Appendix
681 3 in Supplementary Material and Table 1 for names of sampling locations.

682

683







689

690

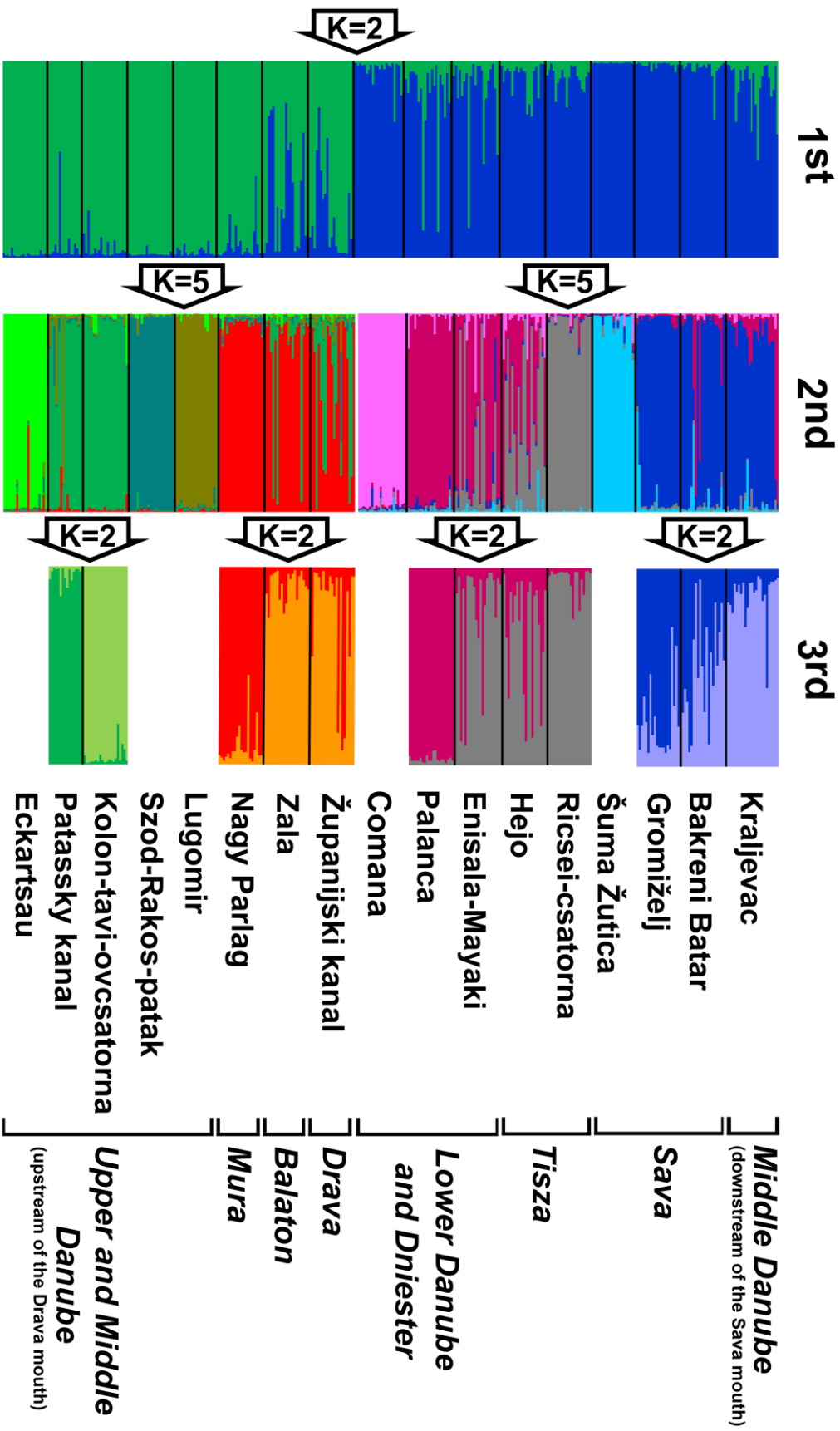
691

692

693

694

695



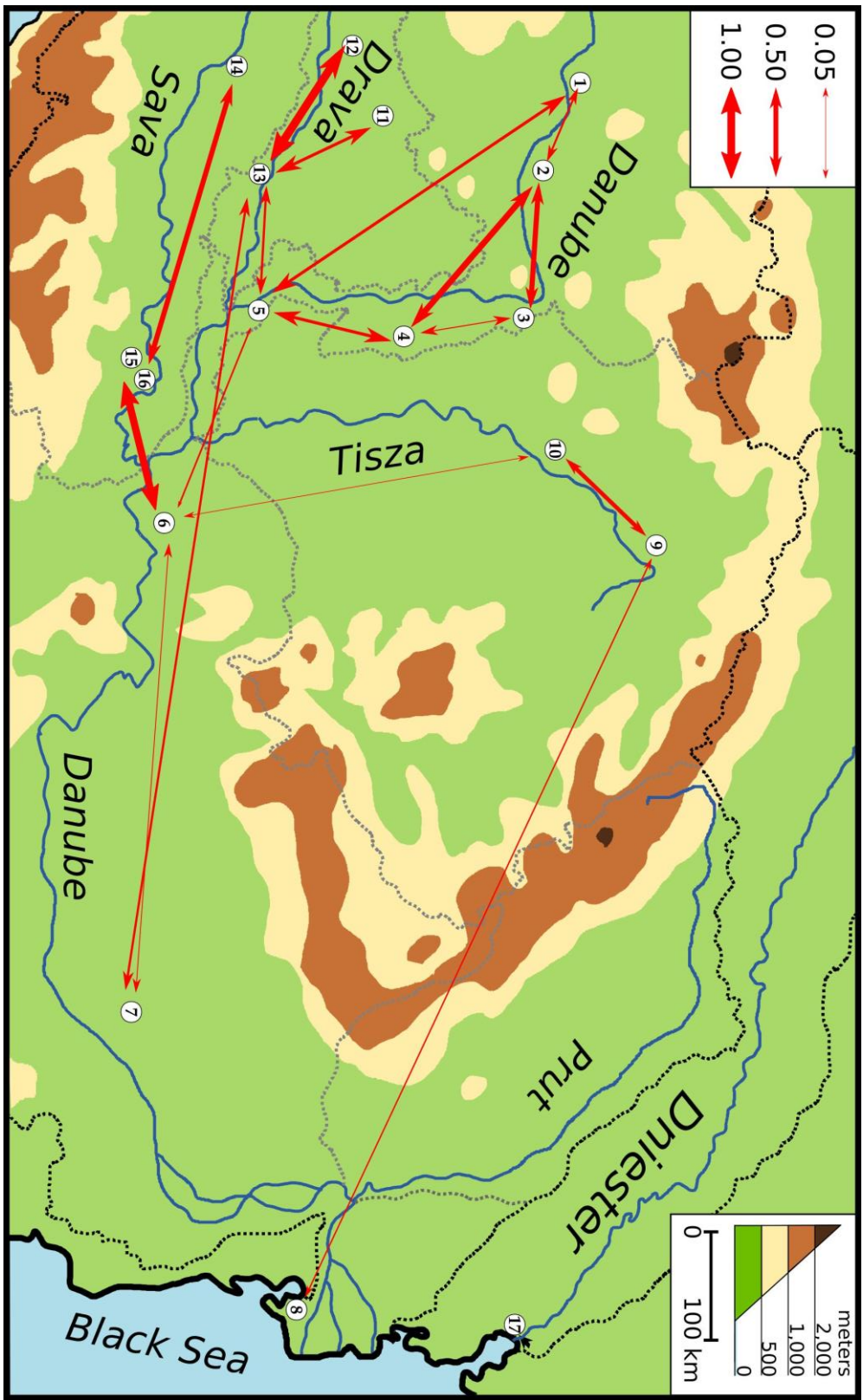


Table 1. Sample locations with a summary of mtDNA haplotype frequencies, diversity and microsatellite genetic diversity: N, number of individuals; H_E, expected heterozygosity in the population; H_O, observed heterozygosity; F_{IS}, values showed no statistically significant deviations from HWE (P < 0.001); Ar, allelic richness; Pr, private alleles; θ, average values of effective population sizes calculated from IM model estimations (Original IM model estimates are listed in Appendix 1), considerable deviation between estimations was observed for Županijski kanal (*), Lower Sava locations are considered together.

Location	Drainage, system	Country	Coordinates	mtDNA – Haplotype frequency											Microsatellite DNA							
				N	Da1	Da2	Da3	Da4	Da5	Da6	Ti1	Ti2	Sa1	Da7	N	H _E	H _O	F _{IS}	Ar	Pr	θ	
1. Eckartsau	Upper Danube	Austria	48° 08' 23" N 16° 47' 21" E	10	10											20	0.523	0.500	0.071	4.37 ± 0.88	0.07 ± 0.07	0.80
2. Patašský kanál	Middle Danube	Slovakia	47° 52' 48" N 17° 38' 34" E	11	9		2									15	0.684	0.724	- 0.024	5.57 ± 0.78	~ 0	1.48
3. Sződ-Rákos-patak	Middle Danube	Hungary	47° 37' 33" N 19° 17' 46" E	10			10									20	0.515	0.564	- 0.071	4.29 ± 0.61	~ 0	1.08
4. Kolon-tavi-övesatorna	Middle Danube	Hungary	46° 45' 00" N 19° 18' 18" E	10	10											20	0.676	0.693	0.000	6.86 ± 1.22	~ 0	3.22
5. Lugomir	Middle Danube	Serbia	45° 46' 33" N 19° 00' 04" E	10	9	1										19	0.634	0.639	0.020	5.96 ± 1.12	~ 0	1.71
6. Kraljevac	Middle Danube	Serbia	44° 51' 07" N 20° 58' 57" E	10	5		3							2		24	0.762	0.798	- 0.026	9.29 ± 1.48	~ 0	8.37
7. Comana	Lower Danube	Romania	44° 09' 53" N 26° 06' 23" E	12						12						22	0.537	0.513	0.067	5.14 ± 1.35	~ 0	1.80
8. Enisala	Danube Delta	Romania	44° 53' 25" N 28° 50' 30" E	12			1	1	1	9						21	0.797	0.819	- 0.003	11.14 ± 1.85	0.64 ± 0.20	44.78
9. Ricsei-csatorna	Upper Tisza	Hungary	48° 20' 11" N 21° 57' 58" E	10							8	2				20	0.675	0.721	- 0.043	6.71 ± 1.15	~ 0	2.24
10. Hejő	Middle Tisza	Hungary	47° 51' 58" N 21° 00' 15" E	10								10				20	0.743	0.764	- 0.004	9.00 ± 1.29	0.33 ± 0.22	12.09
11. Zala	Balaton	Hungary	46° 42' 07" N 17° 15' 30" E	10						10						20	0.743	0.786	- 0.032	8.43 ± 1.63	0.20 ± 0.17	1.45
12. Nagy Parlag	Mura	Slovenia	46° 31' 55" N 16° 25' 51" E	10						10						20	0.578	0.607	- 0.024	6.29 ± 1.61	~ 0	1.25
13. Županijski kanal	Drava	Croatia	45° 52' 33" N 17° 32' 13" E	16						16						20	0.711	0.693	0.051	8.86 ± 1.50	0.04 ± 0.03	5.87*
14. Šuma Žutica	Middle Sava	Croatia	45° 37' 56" N 16° 26' 42" E	11										11		19	0.378	0.331	0.152	3.43 +/- 1.13	~ 0	0.40
15. Gromiželj	Lower Sava	Bosnia and Herzegovina	44° 51' 58" N 19° 18' 29" E	10										10		20	0.678	0.686	0.015	8.14 ± 1.40	0.19 ± 0.11	2.81
16. Bakreni Batar	Lower Sava	Serbia	44° 55' 45" N 19° 28' 34" E	10										10		20	0.766	0.779	- 0.009	8.14 ± 1.34	0.14 ± 0.11	
17. Palanca-Mayaki	Dniester Delta	Moldova/Ukraine	46° 25' 12" N 30° 07' 30" E	10						5				5		21	0.776	0.816	- 0.028	10.91 ± 1.93	1.63 ± 0.61	25.10
				182	43	1	16	1	1	62	18	2	33	5	341							

Table 2. List of species with associated Genbank accession numbers and references for each species used in the molecular clock analysis.

Species	GenBank	Reference
<i>Umbra limi</i> (Kirtland, 1840)	AY497458	Grande et al. (2004)
<i>Umbra pygmaea</i> (DeKay, 1842)	NC_022456	Campbell et al. (2013)
<i>Dallia pectoralis</i> Bean, 1880	NC_004592	Ishiguro et al. (2003)
<i>Novumbra hubbsi</i> Schultz, 1929	AY497457	Grande et al. (2004)
<i>Esox lucius</i> Linnaeus, 1758	KM281478	Skog et al. (2014)
<i>Esox niger</i> Lesueur, 1818	AY497441	Grande et al. (2004)

Table 3. Paired values of F_{ST} above and D_{AS} below the diagonal for microsatellite marker data.

** $P < 0.01$; *** $P < 0.001$; NS non-significant after Bonferroni-type correction.

	1	2	3	4	5	6	7	8	9	10	11	12	13	14	15	16	17
1. Eckartsau		0.282***	0.346***	0.240***	0.319***	0.263***	0.355***	0.222***	0.303***	0.231***	0.218***	0.278***	0.239***	0.514***	0.349***	0.278***	0.219***
2. Patašský kanál	0.633		0.265***	0.121***	0.131***	0.107***	0.261***	0.097***	0.192***	0.133***	0.126***	0.232***	0.085***	0.420***	0.244***	0.152***	0.127***
3. Szód-Rákos-patak	0.588	0.566		0.340***	0.275***	0.261***	0.352***	0.167***	0.213***	0.184***	0.222***	0.247***	0.200***	0.513***	0.355***	0.261***	0.191***
4. Kolon-tavi-övsatorna	0.509	0.324	0.764		0.180***	0.165***	0.329***	0.182***	0.248***	0.209***	0.151***	0.267***	0.162***	0.416***	0.251***	0.187***	0.207***
5. Lugomir	0.680	0.318	0.532	0.452		0.176***	0.333***	0.159***	0.197***	0.219***	0.200***	0.272***	0.152***	0.437***	0.276***	0.194***	0.203***
6. Kraljevac	0.695	0.357	0.697	0.515	0.506		0.176***	0.068***	0.160***	0.103***	0.098***	0.204***	0.082***	0.281***	0.127***	0.038***	0.082***
7. Comana	0.672	0.582	0.646	0.761	0.735	0.425		0.144***	0.212***	0.150***	0.138***	0.228***	0.185***	0.429***	0.306***	0.219***	0.133***
8. Enisala	0.609	0.356	0.435	0.623	0.496	0.288	0.360		0.069***	0.022**	0.053***	0.117***	0.037***	0.322***	0.165***	0.081***	0.041***
9. Ricsei-csatorna	0.710	0.581	0.437	0.697	0.500	0.551	0.479	0.259		0.078***	0.114***	0.189***	0.141***	0.407***	0.238***	0.163***	0.121***
10. Hejő	0.554	0.453	0.433	0.646	0.649	0.408	0.352	0.108	0.254		0.058***	0.152***	0.093***	0.355***	0.194***	0.121***	0.044***
11. Zala	0.528	0.396	0.534	0.435	0.569	0.358	0.321	0.237	0.381	0.228		0.115***	0.065***	0.376***	0.199***	0.123***	0.065***
12. Nagy Parlag	0.531	0.561	0.404	0.634	0.601	0.581	0.382	0.344	0.455	0.410	0.296		0.096***	0.477***	0.303***	0.226***	0.130***
13. Županijski kanal	0.552	0.265	0.430	0.447	0.397	0.283	0.378	0.149	0.451	0.337	0.222	0.215		0.390***	0.229***	0.121***	0.069***
14. Šuma Žutica	0.915	0.826	0.869	0.832	0.836	0.588	0.656	0.701	0.786	0.722	0.787	0.863	0.781		0.213***	0.208***	0.348***
15. Gromiželj	0.842	0.723	0.839	0.721	0.739	0.381	0.667	0.548	0.654	0.582	0.596	0.739	0.687	0.356		0.028NS	0.195***
16. Bakreni Batar	0.741	0.521	0.679	0.613	0.590	0.121	0.516	0.329	0.535	0.450	0.455	0.622	0.409	0.404	0.075		0.105***
17. Palanca-Mayaki	0.578	0.460	0.486	0.720	0.646	0.363	0.315	0.231	0.461	0.212	0.302	0.363	0.271	0.763	0.670	0.423	

Appendix 1. Hierarchical steps in estimating K (the number of genetic clusters) from STRUCTURE runs using the ΔK method. L(K) - posterior probability of K; stdev - standard deviation of L(K) from seven independent runs; ΔK - an *ad hoc* quantity, predictor of the real number of clusters (Evanno et al., 2005), best ΔK are highlighted.

	K	L(K)	stdev	ΔK
1 st step -All samples	1	-10776	0.34	
	2	-10108	3.61	77.70
	3	-9720.13	29.71	3.82
	4	-9445.66	56.36	0.66
	5	-9208.26	34.05	2.68
	6	-9061.96	45.16	0.37
	7	-8898.97	30.91	0.43
	8	-8722.77	28.21	3.04
	9	-8632.27	97.58	3.67
	10	-8900.31	320.25	1.64
	11	-8643.01	130.96	2.02
	12	-8649.77	279.43	0.14
	13	-8616.57	246.79	0.78
	14	-8775.64	308.46	0.51
	15	-8778	300.32	0.75
	16	-9005.77	375.83	0.08
	17	-9204.33	333.26	0.26
	18	-9316.57	376.91	
2 nd step – Upper and Middle Danube (upstream of the Drava mouth) and Drava	1	-4287.27	0.26	
	2	-3988.03	0.67	151.06
	3	-3790.39	3.31	14.47
	4	-3640.6	24.60	0.92
	5	-3468.09	0.81	313.65
	6	-3548.07	314.39	0.70
	7	-3407.96	120.50	1.21
	8	-3413.83	22.82	7.63
	9	-3593.76	75.99	
2 nd step – Middle Danube (downstream of the Sava mouth),	1	-5769.64	0.38	

Sava, Tisza, Lower Danube and Dniester	2	-5410.06	4.29	45.03
	3	-5243.7	18.48	0.65
	4	-5065.39	22.48	0.42
	5	-4877.66	0.88	344.92
	6	-4991.84	313.23	0.66
	7	-4900.21	144.59	0.70
	8	-4910.5	35.42	4.31
	9	-5073.56	58.85	0.29
	10	-5253.93	140.44	
	<hr/>			
3 rd step – Patašký kanál & Kolon-tavi-övcatorna	1	-845.73	0.31	
	2	-786.16	1.16	198.61
	3	-956.74	357.87	0.85
	4	-821.37	7.74	26.50
	5	-891.17	137.03	
<hr/>				
3 rd step – Nagy Parlag, Zala & Županijski kanal	1	-1583.26	0.21	
	2	-1514.06	1.76	73.92
	3	-1574.86	13.95	0.89
	4	-1648.09	56.69	1.68
	5	-1816.5	69.77	3.03
	6	-1773.29	44.71	
<hr/>				
3 rd step – Palanca, Enisala, Hejő & Ricsei-csatorna	1	-2592.87	0.5	
	2	-2460.3	0.7	543.1
	3	-2707.9	177.57	0.27
	4	-3002.69	193.38	1.77
	5	-2955.97	159.38	0.66
	6	-3013.94	141.24	
<hr/>				
3 rd step – Gromiželj, Bakreni Batar & Kraljevac	1	-1750.63	0.67	
	2	-1725.3	4.40	13.88
	3	-1761.11	8.35	2.30
	4	-1816.14	20.34	0.73
	5	-1886.04	39.02	0.21
	6	-1964.29	53.17	

Appendix 2. IM model estimates of effective population sizes with 95% highest posterior density (HPD) interval. A single migration parameter was calculated for each population pair. See Table 1 for names of sampling locations. ? – upper boundary for population size could not be calculated due to insufficient prior range.

Sampling sites	DANUBE								TISZA		DRAVA-BALATON			SAVA		DNIESTER
	1	2	3	4	5	6	7	8	9	10	11	12	13	14	15 & 16	17
1		0.70 (0.30 – 1.46)			0.90 (0.30 – 2.90)											
2	1.54 (0.62 – 3.18)		1.24 (0.52 – 2.84)	1.59 (0.81 – 3.15)												
3		0.68 (0.28 – 1.72)		1.23 (0.57 – 2.25)						1.35 (0.63 – 2.43)						
4		3.03 (1.53 – 5.73)	3.51 (1.83 – 6.09)		2.85 (1.17 – 5.25)					3.47 (1.76 – 5.90)						
5	1.90 (0.70 – 4.30)			1.47 (0.57 – 2.91)			1.73 (0.83 – 3.08)						1.75 (0.65 – 3.25)			
6					7.23 (3.78 – 12.93)		9.56 (5.96 – 15.56)			9.83 (6.38 – 15.62)					6.85 (3.85 – 11.25)	
7						2.36 (1.08 – 4.04)		2.20 (1.00 – 6.20)					0.85 (0.25 – 2.65)			
8							58.60 (25.80 – 368.60)		39.40 (20.60 – 400.00?)	41.40 (12.60 – 265.00)						39.70 (21.10 – 74.70)
9								2.60 (1.40 – 7.00)		1.88 (0.76 – 3.96)						
10			11.31 (6.87 – 19.29)	10.85 (5.99 – 17.77)			11.03 (7.03 – 19.82)				13.88 (5.80 – 71.88)					
11													1.45 (0.55 – 9.95)			
12													1.25 (0.35 – 3.55)			
13					8.55 (3.25 – 22.35)		4.15 (1.05 –					2.05 (0.65 – 13.25)	4.95 (1.25 – 15.25)		9.65 (5.85 – 15.25)	

	13.25)				
14	3.66		0.55 (0.25 – 1.65)	0.25 (0.15 – 1.35)	
15 & 16	(1.33 - 8.55)			1.95 (0.85 – 10.75)	
17	25.10 (15.10 – 43.50)				

Appendix 3. IM model estimates of migration rates and times since divergence with 95% highest posterior density (HPD) interval. Migration rates are in bold and above the main diagonal, while times since divergence are in italic and below the diagonal. A single migration parameter was calculated for each population pair. See Table 1 for names of sampling locations. ? – upper boundary of a parameter could not be calculated due to insufficient prior range; ?? – the time of split could not be properly inferred.

Sampling sites	DANUBE								TISZA		DRAVA-BALATON			SAVA		DNIESTER
	1	2	3	4	5	6	7	8	9	10	11	12	13	14	15 & 16	17
1		0.21 (0.00 – 0.82)			0.33 (0.00 – 0.85)											
2	<i>0.22</i> (<i>0.05</i> – <i>3.47</i>)		0.56 (0.14 – 2.57)	0.66 (0.22 – 1.69)												
3		<i>0.28</i> (<i>0.06</i> – <i>2.31</i>)		0.11 (0.02 – 0.31)						0.00 (0.00 – 0.28)						
4		<i>0.23</i> (<i>0.23</i> – <i>20.00?</i>)	<i>0.74</i> (<i>0.35</i> – <i>15.00?</i>)		0.34 (0.00 – 0.90)					0.05 (0.00 – 0.12)						
5	<i>0.25</i> (<i>0.05</i> – <i>30.00?</i>)			<i>0.26</i> (<i>0.05</i> – <i>10.00?</i>)		0.18 (0.00 – 0.48)							0.24 (0.00 – 0.71)			
6				<i>0.47</i> (<i>0.08</i> – <i>10.00?</i>)			0.09 (0.03 – 0.25)			0.07 (0.00 – 0.17)					0.80 (0.35 – 1.63)	
7						<i>1.61</i> (<i>1.18</i> – <i>8.00?</i>)		0.01 (0.00 – 0.25)					0.24 (0.00 – 1.41)			
8							<i>2.29</i> (<i>0.97</i> – <i>5.89</i>)			0.15 (0.00 – 0.55)	0.03 (0.00 – 0.30)					0.00 (0.00 – 0.06)
9								<i>0.36</i> (<i>0.10</i> – <i>0.38</i>)			0.45 (0.00 – 1.78)					
10			<i>0.37</i> (<i>0.19</i> – <i>20.00?</i>)	??		<i>5.47</i>	<i>1.65</i> – <i>20.00?</i>	<i>0.53</i> – <i>30.00?</i>		<i>0.18</i> (<i>0.02</i> – <i>10.00</i>)						
11													0.33 (0.00 – 2.23)			
12													0.89 (0.10 – 2.31)			
13					<i>0.27</i> (<i>0.05</i> – <i>20.00?</i>)		<i>1.45</i> (<i>1.03</i> –					<i>0.71</i> (<i>0.39</i> – <i>10.00?</i>)	<i>0.59</i> (<i>0.23</i> – <i>20.00?</i>)		0.04 (0.00 – 0.13)	

		20.00?)			
14		3.66		??	0.56 (0.21 – 2.76)
15 & 16		(1.33 - 8.55)			0.06 (0.02 – 5.68)
17		5.61 (3.25 – 7.81)			

Appendix 4: IM model estimation of migration rates in individuals per generation with 95% highest posterior density (HPD) interval. See Table 1 for names of sampling locations. + receiving populations.

Sampling sites	DANUBE								TISZA		DRAVA-BALATON			SAVA		DNIESTER
	1+	2+	3+	4+	5+	6+	7+	8+	9+	10+	11+	12+	13+	14+	15 & 16+	17+
1		0.15 (0.00 – 0.60)			0.28 (0.00 – 0.73)											
2	0.08 (0.00 – 0.33)		0.30 (0.08 – 1.39)	1.06 (0.35 – 2.72)												
3		0.41 (0.10 – 1.88)		0.18 (0.03 – 0.50)						0.00 (0.00 – 1.69)						
4		0.48 (0.16 – 1.23)	0.06 (0.01 – 0.17)		0.29 (0.00 – 0.77)					0.30 (0.00 – 0.73)						
5	0.13 (0.00 – 0.34)			0.55 (0.00 – 1.45)		0.75 (0.00 – 2.01)							0.70 (0.00 – 2.08)			
6					0.15 (0.00 – 0.41)		0.08 (0.02 – 0.23)			0.42 (0.00 – 1.03)					1.12 (0.49 – 2.29)	
7						0.38 (0.13 – 1.05)		0.23 (0.00 – 5.6)					0.70 (0.00 – 4.14)			
8							0.01 (0.00 – 0.23)		0.17 (0.00 – 0.62)	0.18 (0.00 – 1.81)						0.00 (0.00 – 0.75)
9								3.36 (0.00 – 12.31)		2.72 (0.00 – 10.76)						
10			0.00 (0.00 – 0.15)	0.08 (0.00 – 0.20)		0.29 (0.00 – 0.71)				0.51 (0.00 – 1.99)						
11													0.97 (0.00 – 6.55)			
12													2.61 (0.29 – 6.78)			
13					0.21 (0.00 – 0.61)		0.22 (0.00 – 1.27)					0.24 (0.00 – 1.62)	0.56 (0.06 – 1.44)		0.01 (0.00 – 0.03)	
14													0.12 (0.00 – 0.30)		0.79 (0.30 – 1.27)	

15 & 16	3.35 (1.46 - 6.82)		0.38)	3.88)	
17		0.00 (0.00 - 1.34)		0.11 (0.04 - 0.55)	